Materials Advances

ROYAL SOCIETY OF CHEMISTRY

PAPER

View Article Online
View Journal | View Issue

Cite this: *Mater. Adv.*, 2024, 5, 4221

Gold nanoparticle-loaded MoS_2 nanosheets with peroxidase-like and pyranose oxidase-like activities for bio-enzyme-free visual detection of glucose, xylose and galactose†

Shilan Fu,‡[ab] Junfeng Liu,[a] Siqi Wu,[a] Lin Zhang,[a] Xu Zhang*[a] and FengFu Fu *[a]

Enzyme mimics with dual enzyme-like activities can catalyse cascade reactions with high efficiency and thus play a significant role in biochemistry since multistep cascade reactions often occur in biocatalysis. Especially, a nanozyme that simultaneously possesses peroxidase-like and pyranose oxidase (POx)-like activities is highly desired since it can be used for bio-synthetizing rare sugars and fabricating bio-enzyme-free colorimetric methods for the detection of various pyranoses. We herein prepared a novel dual-active nanozyme, which simultaneously possesses enhanced and stable peroxidase-like and POx-like activities, by loading gold nanoparticles (AuNPs) on MoS_2 nanosheets (AuNPs@MoS_2). The prepared AuNPs@MoS_2 nanozyme can catalyse various tandem reactions of pyranose oxidation and H_2O_2-mediated oxidation of TMB with high efficiency and, therefore, can be used to fabricate bio-enzyme-free colorimetric methods for the detection of various monosaccharides with a pyranyl ring, including glucose, xylose and galactose. Based on the AuNPs@MoS_2 nanozyme, we successfully developed bio-enzyme-free colorimetric methods for the detection of glucose, xylose and galactose with a visual detection limit of 0.2–0.3 mM and a spectrometry detection limit of 5.0–11 μM. The developed colorimetric glucose, xylose and galactose detection methods were successfully used to detect glucose in serum, xylose in bread and galactose in milk, respectively, with a recovery of 89–108% and a relative standard deviation (RSD, n = 5) of <5%. With enhanced peroxidase-like and POx-like activities and good stability, the developed AuNPs@MoS_2 provided a promising dual-active nanozyme for the bio-enzyme-free catalysis of various cascade reactions for the oxidation of various monosaccharides with a pyranyl ring and for further fabricating bio-enzyme-free, cost-effective and simple colorimetric sensors for the visual detection of various monosaccharides with a pyranyl ring, including glucose, xylose and galactose.

Received 30th January 2024,
Accepted 26th March 2024

DOI: 10.1039/d4ma00086b

rsc.li/materials-advances

1. Introduction

Natural enzymes play a key role in biochemistry because they can catalyse various biochemical reactions with high specificity and activity under mild conditions.[1] However, the intrinsic drawbacks of natural enzymes, such as thermal instability, a higher cost of preparation/purification and limited natural sources, restrict their practical application.[2] Compared with natural enzymes, artificial enzyme mimics, especially catalytically active nanomaterials (known as nanozymes), possess intrinsic advantages such as a lower cost of preparation, better thermal stability, tunable catalytic activity, and similar or higher catalytic activity and specificity.[3,4] Accordingly, the discovery and development of nanozymes have attracted great research attention in recent years. Along this goal, a lot of nanozymes with different enzyme-like activities such as peroxidase-like activity,[5–9] catalase-like activity,[10,11] and glucose oxidase (GOx)-like activity,[12–17] have been prepared and used for fabricating colorimetric detection methods for various small molecules. Unfortunately, these previously reported nanozymes possess only one enzyme-like activity and thus could not be used for bio-enzyme-free catalysis of cascade reactions, in which the product of a reaction is a substrate for another reaction. For example, nanozymes with peroxidase-like activity cannot be directly used for fabricating a colorimetric detection method for glucose without natural GOx,[5–9] whereas nanozymes with GOx-like activity cannot be

[a] *Key Laboratory for Analytical Science of Food Safety and Biology of MOE, Fujian Provincial Key Lab of Analysis and Detection for Food Safety, College of Chemistry, Fuzhou University, Fuzhou, Fujian 350116, China. E-mail: 1959392119@qq.com, fengfu@fzu.edu.cn*

[b] *College of Chemistry and Materials Science, Fujian Normal University, Fuzhou, Fujian 350117, China*

† Electronic supplementary information (ESI) available. See DOI: https://doi.org/10.1039/d4ma00086b

‡ Current addresses: School of Chemistry and Chemical Engineering, Shanghai Jiao Tong University, Shanghai 200240, China.

directly used for fabricating a colorimetric detection method for glucose without natural horseradish peroxidase (HRP).[12–14] In fact, a multistep cascade reaction is a common phenomenon and often occurs in biocatalysis.[18–20] Thus, the discovery and development of nanozymes with dual enzyme-like activities, which can catalyse cascade reactions with high efficiency, have attracted much attention and become a major challenge in biomimetic catalysis.

To realize the bio-enzyme-free catalysis of the cascade reactions, one effective method is to prepare hybrid nanomaterials with dual enzyme-like activities.[10,21,22] So far, some nanozymes with dual enzyme-like activity have been prepared by integrating different materials together, such as Au hydrogel with a well-defined nanowire network,[23] CeO_2-encapsulated hollow Ag–Au nanocage,[24] mesoporous silica-encapsulated gold nanoparticles (AuNPs),[25,26] modified carbon nitride and so on.[27–33] However, most of the previous dual enzyme-like nanozymes mainly possessed both peroxidase-like activity and GOx-like activity, and the nanozymes simultaneously possessing peroxidase-like activity and other sugar oxidase-like activity, such as pyranose oxidase (POx)-like activity have been seldom reported until now. POx is an oxidoreductase that can catalyse the oxidation of several monosaccharides with pyranyl ring, including glucose, xylose and galactose,[34] which make it potentially useful in the biosynthesis of rare sugars, carbohydrate bio-transformation and bio-sensing.[35] Therefore, the discovery and development of nanozymes with peroxidase-like activity and POx-like activity simultaneously are highly desired for developing the bio-enzyme-free colorimetric detection method of various monosaccharides, including glucose, xylose and galactose. In this study, we developed a nanozyme with enhanced peroxidase-like activity and POx-like activity simultaneously by loading AuNPs on MoS_2 nanosheets in order to provide a stable and highly efficient dual-active nanozyme for catalysing the cascade reactions of various monosaccharides with pyranyl ring, and further for fabricating bio-enzyme-free colorimetric sensor for the visual detection of various monosaccharides with pyranyl ring including glucose, xylose and galactose.

2. Experimental section

2.1. Materials and apparatus

The MoS_2 powder (>98%, CAS No.: 1317-33-5), chloroauric acid tetrahydrate ($HAuCl_4{\cdot}4H_2O$) and horseradish peroxidase (HRP, specific activity > 180 U mg^{-1}) were purchased from Aladdin Company (Shanghai, China). Glucose oxidase (GOx, specific activity > 100 U mg^{-1}) was purchased from Sangon Biotech Co., Ltd (Shanghai, China). The GA-3 glucose meter was obtained from Sinocare Company (Changsha, Hunan of China). The acetic acid/sodium acetate buffer (200 mM, pH 4.6) was prepared by mixing 200 mM of $CH_3CO_2Na{\cdot}3H_2O$ and CH_3COOH. Other materials and apparatus used in the experiment are summarized in ESI.†

2.2. Preparation of AuNPs-loaded MoS_2 nanosheets with peroxidase-like and POx-like activities

Firstly, the MoS_2 nanosheets were prepared, referring to the previous method.[36] About 25.0 mg of MoS_2 powder was weighted and dispersed in 10 mL water in a centrifuge tube, and then the whole was ultrasonically treated for 4 h at 20 °C, 80 KHz and 300 W to obtain MoS_2 nanosheets. Subsequently, the obtained MoS_2 nanosheet dispersion was separated and collected by centrifuging the whole mixture for 10 min at 20 °C and 5000 rpm to discard the sediment in the bottom. The concentration of MoS_2 nanosheet dispersion was quantified by detecting the Mo concentration with inductively coupled plasma mass spectrometry (ICP-MS).

In a centrifuge tube, 2.0 mL of the above MoS_2 nanosheet dispersion (the concentration was adjusted to 11.0 μg MoS_2/mL with water) was added, and then 20 μL of 2% $HAuCl_4$ solution was added under 500 rpm agitation. The whole dispersion was further ultrasonically treated for 10 min at 20 °C, 45 KHz and 300 W, and then 150 μL of fresh $NaBH_4$ solution (0.05 M) was fleetly added, followed by 5 min agitation of 500 rpm. Finally, 200 μL of 0.01 M sodium citrate solution was fleetly added, and the whole mixture was continuously agitated for 30 min at 500 rpm to obtain AuNPs-loaded MoS_2 nanosheet (AuNPs@MoS_2) dispersion. The obtained AuNPs@MoS_2 dispersion was stored at 5 °C and used within one month.

2.3. Dual enzyme-like activities and characterization of the prepared AuNPs@MoS_2

(1) Peroxidase-like activity characterization of AuNPs@MoS_2. The peroxidase-like activity of the prepared AuNPs@MoS_2 was investigated by directly using AuNPs@MoS_2 to catalyse H_2O_2-mediated oxidation of 3,3′,5,5′-tetramethylbenzidine (TMB). Concretely, 10 μL of the above prepared AuNPs@MoS_2 dispersion was fully mixed with 20 μL of 0.2 M H_2O_2, 15 μL of 5.0 mM TMB and 55 μL of acetic acid/sodium acetate buffer in a 0.2 mL vial. After a reaction of 30 min under room temperature, the colour of the solution was recorded with a camera, and the absorption spectrum of the solution was measured with a microplate reader in the range of 500–800 nm simultaneously. The comparative analysis of peroxidase-like activity toward TMB and H_2O_2 between AuNPs@MoS_2 and natural HRP was performed by determining their steady-state kinetic parameters to objectively evaluate the peroxidase-like activity of AuNPs@MoS_2. The Michaelis–Menten parameters, including K_m and V_{max} were calculated based on the Lineweaver–Burk plot: $1/V = K_m/V_{max}(1/[C] + 1/K_m)$, where V and V_{max} are the initial and the maximal reaction velocity respectively, [C] is the substrate concentration and K_m is the Michaelis constant.

(2) Pyranose oxidase (POx)-like activity characterization of AuNPs@MoS_2. The POx-like activity of the prepared AuNPs@MoS_2 was investigated by directly using AuNPs@MoS_2 to catalyse various pyranose rings, including glucose, xylose and galactose for generating H_2O_2, and then using HRP to catalyse the H_2O_2-mediated oxidation of TMB. Concretely, 30 μL of AuNPs@MoS_2 dispersion was fully mixed with 10 μL of 50 mM glucose, xylose or galactose solution in a 0.2 mL vial. After reaction for 30 min under room temperature, 8 μL of 5.0 mM TMB, 10 μL of 5.0 μg mL^{-1} HRP and 42 μL of acetic acid/sodium acetate buffer were added. The whole solution was gently mixed and then allowed to stand for 10 min under room

temperature; then, the colour of the solution was recorded with a camera and the absorption spectrum of the solution was also measured with a microplate reader in the range of 500–800 nm. The POx-like activity of AuNPs@MoS_2 was objectively evaluated *via* the comparative analysis of the activity toward glucose between AuNPs@MoS_2 and natural GOx since natural POx could not be commercially obtained. Their steady-state kinetic parameters, including K_m and V_{max} were also calculated according to the Lineweaver–Burk plot, like the case of peroxidase-like activity.

2.4. Bio-enzyme-free colorimetric detection of glucose, xylose and galactose based on AuNPs@MoS_2

(1) Colorimetric detection of glucose based on AuNPs@MoS_2. For performing colorimetric detection of glucose based on AuNPs@MoS_2 dual-active nanozyme, 50 μL AuNPs@MoS_2 dispersion was fully mixed with 10 μL glucose standard or sample solution and 40 μL water in a vial. Then, the mixture was incubated for 20 min under 500 rpm agitation and at room temperature. Subsequently, 3.2 μL of 5.0 mM TMB, 40 μL of acetic acid/sodium acetate buffer and 56.8 μL of water were added in order, and the mixture was incubated for 40 min under 40 °C. The colour of the solution was recorded with a camera, and the absorption spectrum of the solution was also measured with a microplate reader in the range of 500–800 nm. The concentration of glucose was quantified based on the absorbance of the solution at 652 nm (A_{652}) or the solution colour with naked-eye observation.

(2) Colorimetric detection of xylose and galactose based on AuNPs@MoS_2. The xylose and galactose were detected using the same procedure. Concretely, 40 μL of AuNPs@MoS_2 dispersion was fully mixed with 10 μL xylose/galactose standard or sample solution and 50 μL of water in a vial. Then, the mixture was incubated for 20 min under 500 rpm agitation and room temperature. Subsequently, 10 μL of 12 mM TMB, 40 μL of acetic acid/sodium acetate buffer and 50 μL of water were added in order, and the mixture was incubated for 40 min under 40 °C. The colour of the solution was recorded with a camera and the absorption spectrum of the solution was also measured with a microplate reader in the range of 500–800 nm. The concentration of xylose or galactose was quantified based on the absorbance of the solution at 652 nm (A_{652}) or the solution colour with bare-eye observation.

2.5. Determination of glucose in serum, xylose in bread and galactose in milk samples

The glucose in the serum was detected to confirm the reliability of the developed colorimetric glucose detection method. The serum sample was pre-treated by adding 450 μL acetonitrile and 200 μL water into 100 μL of serum, which was followed by 10 min of centrifugation (10 000 rpm) to remove the protein. The solution was then diluted with water to 5.0 mL (a total 50-fold dilution), and the glucose in the final solution was detected according to the above procedure. The serum spiked with different concentrations of glucose was also pre-treated and detected in the same manner to obtain recovery. The analytical result obtained with our method was compared with that obtained with a commercial glucose meter.

The xylose in bread and the galactose in milk were detected to verify the reliability of the developed colorimetric xylose and galactose detection method, respectively. The xylose in 2.0 g of bread was extracted with 5.0 mL water for 30 min under full agitation, and then the supernatant was separated and collected by centrifugation for 10 min at 10 000 rpm. The residue was repeatedly extracted once again in the same manner, and the two extracts were combined. The xylose in the final extract was then detected according to the above procedure after it was diluted 20-fold with water, and the bread spiked with xylose was also pre-treated and detected in the same manner to obtain recovery. The milk was pre-treated by mixing 1.6 mL of milk with 2.5 mL water, 0.7 mL of 10% trichloroacetic acid and 1.0 mL of chloroform, followed by 15 min of ultra-sonication and 10 min of centrifugation (12 000 rpm) to remove protein and fat. The galactose in the supernatant was then detected according to the above procedure after it was diluted 20-fold with water, and the milk spiked with galactose was also pre-treated and detected in the same manner to obtain recovery.

3. Results and discussion

3.1. Experimental strategy and characterization of the prepared AuNPs@MoS_2 nanozyme

The detailed experimental strategy for preparing AuNPs@MoS_2 with enhanced peroxidase-like and POx-like activities and for developing bio-enzyme-free colorimetric detection methods of glucose, xylose and galactose based on AuNPs@MoS_2 are shown in Scheme 1. As mentioned above, many previous studies have reported that nano-MoS_2, including MoS_2 nanosheets and nano-flowers, possess peroxidase-like activity,[37,38] and the "non-naked" AuNPs may show dual enzyme-like activities such as peroxidase-like and GOx-like activities at the same pH.[28] It was also reported that the introduction of various nanosheets such as MoS_2, g-C_3N_4 and graphene oxide (GO) can more effectively disperse noble metal nanoparticles on the surface of nanosheets and thus enhance the enzyme-like activities of both nanosheets and noble metal nanoparticles.[28,39,40] Inspired by the above research and considering the fact that glucose possesses a core

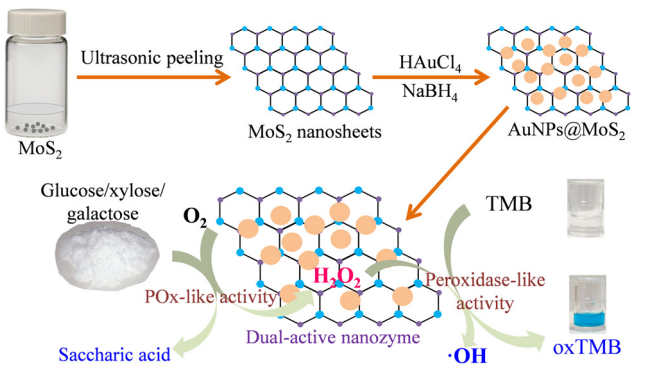

Scheme 1 Illustration of the experimental strategy for preparing AuNPs@MoS_2 with enhanced peroxidase-like and POx-like activities and the bio-enzyme-free colorimetric detection of glucose, xylose and galactose based on AuNPs@MoS_2.

structure of pyranose (pyranyl ring), it is possible to form a nanozyme with enhanced peroxidase-like and POx-like activities simultaneously by well-dispersedly loading AuNPs on MoS_2 nanosheets, which will provide a stable and highly efficient dual-active nanozyme for catalysing the cascade reactions of various pyranose structures, and further developing sensitive and cost-effective bio-enzyme-free colorimetric methods for the visual detection of various pyranose rings, including glucose, xylose and galactose.

The characterizations using transmission electron microscopy (TEM), atomic force microscopy (AFM), energy-dispersive X-ray spectroscopy (EDX), X-ray photoelectron spectroscopy (XPS) and X-ray diffraction (XRD) were performed to verify the successful preparation of AuNPs@MoS_2 nanozyme, as we expected. As the TEM images shown in Fig. 1 and the AFM image shown in Fig. S1 (see ESI†), the MoS_2 nanosheets obtained by ultrasonically stripping MoS_2 powder have an obvious laminated structure with a thickness of ~5 nm and a size of 100–400 nm (Fig. 1A), and a large number of AuNPs with sizes of 5–10 nm and an inter-planar spacing of 0.235 nm (Fig. 1B and C), which is the lattice fringe of Au (111), was well dispersed on the surface.[14] In addition, the EDX mapping images of Mo, S and Au revealed that Mo, S and Au correspondingly distributed on the prepared AuNPs@MoS_2 (Fig. 1E–H). All the above experimental results validated that the AuNPs@MoS_2 nanozyme was successfully synthesized.

The XRD spectra shown in Fig. S2 (see ESI†) also verified the successful preparation of the AuNPs@MoS_2 nanozyme. The prepared AuNPs@MoS_2 nanozyme not only showed the typical peaks of MoS_2 nanosheets at 2θ = 14.2° and 44.3°,[41] but also showed the typical peaks of AuNPs at 38.2°, 64.7° and 77.7°.[28] The chemical states of Au, Mo and S were investigated with XPS, and the Au 4f, Mo 3d and S 2p spectra and their deconvoluted results are shown in Fig. S3 (see ESI†). The deconvoluted Au 4f spectrum had two major peaks corresponding to Au $4f_{7/2}$ (82.9 eV) and Au $4f_{5/2}$ (86.6 eV), suggesting the Au^0 state of the loaded AuNPs.[42] The Mo 3d spectrum displayed two peaks at 232.5 eV and 235.6 eV, corresponding to Mo $3d_{3/2}$ and Mo $3d_{5/2}$ of MoS_2 nanosheets, and the S 2p spectrum displayed two peaks at 167.2 eV and 168.3 eV, corresponding to S $2p_{3/2}$ and S $2p_{1/2}$ of MoS_2 nanosheets.[43] The XRD and XPS results further demonstrated that the AuNPs@MoS_2 nanozyme was successfully prepared, as Scheme 1 indicated.

3.2. The peroxidase-like activity and POx-like activity of the prepared AuNPs@MoS_2

As mentioned in the experimental section, the peroxidase-like activity of the prepared AuNPs@MoS_2 nanozyme was verified by catalysing the H_2O_2-mediated oxidation of TMB, and its POx-like activity was verified by catalysing glucose, xylose and galactose for generating H_2O_2 and then further using HRP to catalyse the H_2O_2-mediated oxidation of TMB. From Fig. 2A, it is clearly observed that AuNPs@MoS_2 can effectively catalyse the oxidation of TMB to generate a blue colour with maximum absorption at 652 nm in the presence of H_2O_2 but could not catalyse the oxidation of TMB in the absence of H_2O_2 (blank), verifying that the prepared AuNPs@MoS_2 possessed high peroxidase-like activity, not oxidase-like activity. The results shown in Fig. 2B also reveal that AuNPs@MoS_2 can effectively catalyse the oxidation of glucose, xylose and galactose to generate H_2O_2, and thus lead to the generation of blue colour and a maximum absorption at 652 nm in the mixture of HRP

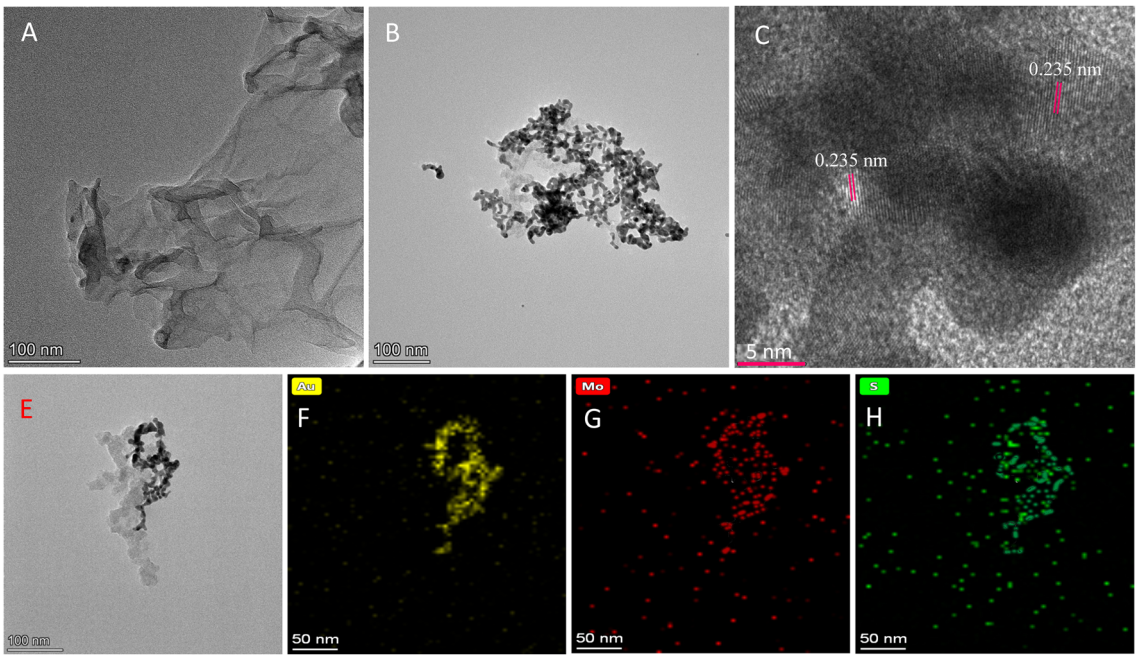

Fig. 1 The TEM image of the prepared MoS_2 nanosheets (A) and AuNPs@MoS_2 (B); the high-resolution TEM (HTEM) image of AuNPs loaded on MoS_2 nanosheets (C); and the EDX mapping images of AuNPs@MoS_2 (E)–(H).

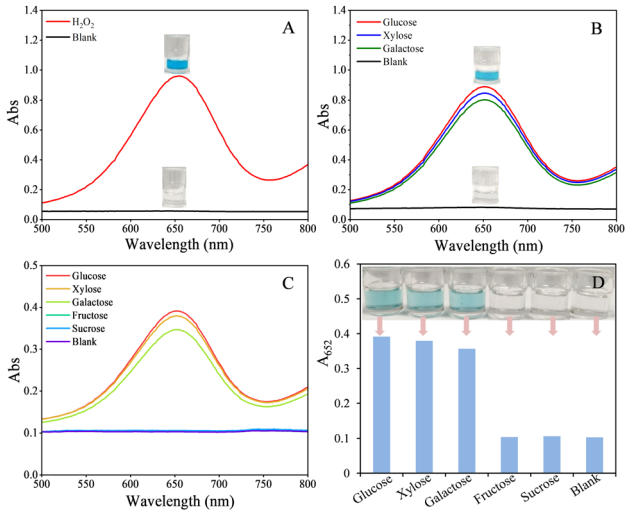

Fig. 2 (A): The absorption spectra and photographs of the mixture of TMB and AuNPs@MoS_2 in the presence and absence of H_2O_2 (blank); (B): absorption spectra and photographs for catalysing the oxidation of pyranose (glucose, xylose and galactose) with AuNPs@MoS_2 and then further catalysing the oxidation of TMB with HRP; (C) and (D): absorption spectra and photographs for directly catalysing the tandem reactions of pyranose (glucose, xylose and galactose)/non-pyranose (fructose and sucrose) oxidation and H_2O_2-mediated oxidation of TMB with AuNPs@MoS_2. The concentrations of pyranose and non-pyranose are all 2.0 mM.

and TMB, indicating that the prepared AuNPs@MoS_2 also possessed high POx-like activity.

The dual enzyme-like activities (peroxidase-like and POx-like activities) and specificity of the AuNPs@MoS_2 nanozyme were further confirmed by directly using AuNPs@MoS_2 to catalyse various cascade reactions, such as the tandem reactions of pyranose (glucose, xylose and galactose) oxidation/non-pyranose (fructose and sucrose) oxidation and H_2O_2-mediated oxidation of TMB, according to the procedure in the experimental section 2.4. As shown in Fig. 2C and D, AuNPs@MoS_2 can high-efficiently catalyse the oxidation of glucose, xylose and galactose to generate H_2O_2 and sequentially catalyse the H_2O_2-mediated oxidation of TMB to generate blue colour in solution, accompanied by a maximum absorption at 652 nm. Whereas, in the case of non-pyranose (fructose and sucrose), the solution was colourless and did not have obvious absorption at 652 nm, indicating that AuNPs@MoS_2 could not catalyse the oxidation of fructose and sucrose to generate H_2O_2, and thus could not further catalyse the H_2O_2-mediated oxidation of TMB to generate blue colour in the solution. The above experimental results verified that the prepared AuNPs@MoS_2 can exhibit peroxidase-like and POx-like activities simultaneously in the same system and has excellent specificity.

The size, thickness and concentration of MoS_2 nanosheets affect the dispersity of AuNPs on the surface of MoS_2 nanosheets, and thus remarkably affect the dual enzyme-like activity and stability of the prepared AuNPs@MoS_2. To obtain AuNPs@MoS_2 with high and stable peroxidase-like and POx-like activity simultaneously, we optimized the size and thickness of MoS_2 nanosheets by controlling the time of ultrasonically stripping MoS_2 powder. As shown in Fig. S4 (see ESI†), a shorter time (3 h) is in favour of obtaining bigger and thicker MoS_2 nanosheets (Fig. S4A, ESI†), which resulted in the prepared AuNPs@MoS_2 sheets having poor dispersity and a low amount of AuNPs (Fig. S4B, ESI†). Thus, the prepared AuNPs@MoS_2 has lower dual enzyme-like activities (Fig. S4C, ESI†). If the time of ultrasonication is too long (6 h), the obtained MoS_2 nanosheets have a very small size (Fig. S4G, ESI†). In this case, the prepared nanozyme is more like the mixture of AuNPs and MoS_2 nanosheets than AuNPs-loaded MoS_2 nanosheets (Fig. S4H, ESI†) and thus has poor stability, although it also has high dual enzyme-like activities (Fig. S4I, ESI†). When the time is 4 h, the obtained MoS_2 nanosheet has a thickness of $\sim$5 nm and a size of 100–400 nm, and the prepared AuNPs@MoS_2 has a good dispersity and appropriate amount of AuNPs (Fig. S4D and E, ESI†). Thus, the prepared AuNPs@MoS_2 has high dual enzyme-like activities and better stability. The concentration of MoS_2 nanosheets was also optimized by detecting Mo with ICP-MS. The results shown in Fig. S5A (see ESI†) revealed the prepared AuNPs@MoS_2 has the highest dual enzyme-like activities when the concentration is 10–12.5 μg mL^{-1}. The $HAuCl_4$ concentration affects the size and amount of AuNPs of the prepared AuNPs@MoS_2 and thus affects its dual enzyme-like activities. Fig. S5B (see ESI†) shows that the prepared AuNPs@MoS_2 has the highest dual enzyme-like activities when $HAuCl_4$ concentration is 2.0%.

Under the above optimal conditions, the stability of the prepared AuNPs@MoS_2 was investigated by directly using AuNPs@MoS_2 to catalyse the tandem reactions of glucose oxidation and H_2O_2-mediated oxidation of TMB. As shown in Fig. S6 (see ESI†), the absorption at 652 nm (A_{652}) of the system did not decrease obviously even if the AuNPs@MoS_2 dispersion was stored at 5 °C for one month, indicating that the prepared AuNPs@MoS_2 has stable dual enzymes-like activities.

The peroxidase-like activity of AuNPs@MoS_2 was objectively evaluated by comparing the steady-state kinetic parameters toward TMB and H_2O_2 between AuNPs@MoS_2 and natural HRP, and the POx-like activity of AuNPs@MoS_2 was evaluated by comparing the steady-state kinetic parameters toward glucose between AuNPs@MoS_2 and natural GOx since natural POx could not be commercially obtained. As shown in Fig. S7, S8 and Table S1 (see ESI†), the K_m of AuNPs@MoS_2 toward H_2O_2 is slightly higher than HRP, but the K_m of AuNPs@MoS_2 toward TMB is slightly lower than HRP, indicating that the prepared AuNPs@MoS_2 has relatively lower affinity toward H_2O_2 substrate but relatively higher affinity toward the TMB substrate compared to HRP. Thus, a relatively higher H_2O_2 but lower TMB are required in order to achieve maximal peroxidase-like activity for AuNPs@MoS_2. The V_{max} of AuNPs@MoS_2 for H_2O_2 and TMB are all about half of those of HRP, revealing that the AuNPs@MoS_2 required a relatively longer time to catalyse H_2O_2-mediated oxidation of TMB.

Fig. S9 and Table S1 (see ESI†) revealed that the K_m of AuNPs@MoS_2 toward glucose is lower than GOx, indicating that the prepared AuNPs@MoS_2 has a higher affinity toward glucose substrate compared to HRP, and thus lower glucose was required to achieve maximal POx-like activity for AuNPs@MoS_2.

The V_{max} value of AuNPs@MoS_2 for glucose was also slightly lower than those of GOx, demonstrating that AuNPs@MoS_2 can catalyse H_2O_2-mediated oxidation of TMB with a similar rate compared to GOx.

All the above experimental results strongly verified that the prepared AuNPs@MoS_2 nanozyme possessed enhanced peroxidase-like and POx-like activities simultaneously and has excellent specificity. Thus, it can be used to catalyse the tandem reactions of pyranose (glucose, xylose and galactose) oxidation and H_2O_2-mediated oxidation of TMB, which provides a promising approach for developing sensitive and cost-effective bio-enzyme-free colorimetric methods for the detection of various pyranose rings, including glucose, xylose and galactose. As mentioned above, so far, some nanozymes with dual enzyme-like activity, such as peroxidase-like and GOx-like activities, which can be used to catalyse the tandem reactions of glucose oxidation and H_2O_2-mediated oxidation of TMB, have been reported.[23–33] However, the nanozymes simultaneously possessing peroxidase-like activity and POx activity have been seldom reported until now. In comparison with the above dual-active nanozymes,[23–33] the dual-active AuNPs@MoS_2 reported in this study not only has similar or enhanced peroxidase-like activity but also has enhanced POx-like activity, which makes it effectively catalyse the tandem reactions of more monosaccharides including glucose, xylose and galactose oxidation and H_2O_2-mediated oxidation of TMB, providing a promising approach for bio-enzyme-free visual detection of glucose, xylose and galactose.

3.3. Bio-enzyme-free colorimetric detection of glucose based on AuNPs@MoS_2

To verify the feasibility of AuNPs@MoS_2 as a nanozyme with both enhanced peroxidase-like and POx-like activities, the AuNPs@MoS_2 was first used to develop bio-enzyme-free colorimetric methods for the visual detection of glucose, as shown in Scheme 1. The feasibility of the experimental strategy was first investigated with UV-visible spectrometry. As shown in Fig. S10 (see ESI†), in the presence of both glucose, TMB and AuNPs@MoS_2, the solution exhibited obvious blue colour and had a maximum absorbance at 652 nm. Whereas, in the presence of TMB and AuNPs@MoS_2 but without glucose, the solution was almost colourless and had no obvious absorbance at 652 nm (see blank in Fig. S10, ESI†). The above facts clearly illustrated that AuNPs@MoS_2 could effectively catalyse the oxidation of glucose to generate H_2O_2 *via* its POx-like activity and then sequentially catalyse the H_2O_2-mediated oxidation of TMB *via* its peroxidase-like activity, which verified that our experimental strategy is feasible.

To obtain the best performance of the developed colorimetric method for the detection of glucose, various parameters, including AuNPs@MoS_2 amount, the reaction temperature and time between AuNPs@MoS_2 and glucose, TMB concentration, and the reaction temperature and time between AuNPs@MoS_2 and TMB were optimized, respectively. As shown in Fig. S11 (see ESI†), the amount of AuNPs@MoS_2 was optimized in the range of 40–70 μL since its amount directly affected the sensitivity of the method by affecting the velocity and completeness of the glucose oxidation and the H_2O_2-mediated TMB oxidation. Experimental results showed the method had the best and most stable sensitivity when AuNPs@MoS_2 amount was in the range of 50–60 μL, and thus 50 μL of AuNPs@MoS_2 was used in this study (Fig. S11A, ESI†). The reaction temperature and time between AuNPs@MoS_2 and glucose will affect the amount of the generated H_2O_2 and thus affect the sensitivity of the method. The results (Fig. S11B and C, ESI†) showed that the reaction temperature does not remarkably affect the sensitivity of the method in the range of 25–45 °C, and thus, the room temperature was selected to simplify the experiment. Simultaneously, the method has the highest and most stable sensitivity when the reaction time is in the range of 10–30 min, and thus 20 min was selected. The concentration of TMB was optimized in the range of 0.02–0.10 mM, and the results showed the method has the highest sensitivity at 0.08 mM of TMB (Fig. S11D, ESI†). The reaction temperature and time between AuNPs@MoS_2 and TMB were optimized in the range of 30–45 °C and 20–60 min, respectively. The results showed (Fig. S11E and F, ESI†) that the method has the highest and most stable sensitivity in the range of 40–45 °C, and thus 40 °C was selected in this study. Simultaneously, the method has the highest and most stable sensitivity when the reaction time is longer than 30 min, and thus 40 min was selected.

Under the above optimal conditions, a series of glucose solutions were detected using the developed method to investigate the analytical performance of the method. From Fig. 3A, it can be clearly observed that the solution changed from colourless to deep blue step by step when the glucose concentration increased from 0.0 mM to 2.5 mM. The colour change of the solution corresponding to 0.3 mM glucose could be clearly identified by naked-eye observation, *i.e.* the visual detection limit of the method is about 0.3 mM for glucose. The absorbance of the system at 652 nm (A_{652}) showed a good linear correlation with the glucose concentration within 0.0–0.70 mM, with a regression equation of $A_{652} = 0.2699 \times C + 0.1178$ ($R^2 = 0.9738$, C is glucose concentration with unit of mM). The detection limit (LOD, $3\sigma/S$) for glucose was calculated to be 11 μM, and the relative standard deviation (RSD, $n = 5$) for the detection of 0.3 mM glucose was calculated to be 4% (Table S2 in ESI†).

To confirm the applicability and the anti-interference ability of the developed colorimetric glucose method, the glucose in the serum was detected with the developed method by considering the fact that the main pyranose in serum is glucose, and the results were compared with that obtained with a commercial glucose meter. The results showed that abundant proteins in the original serum would interfere with the detection of glucose in the original serum, like most nanozyme-based colorimetric methods.[6,37] Thus, the proteins in serum should be simply isolated according to the procedure in experimental section 2.5 before detection. As Table 1 shows, glucose in the pre-treated serum can be detected by the proposed method with a recovery of 89–101% and a RSD ($n = 5$) $< 5\%$, and the results detected with our method are consistent with that detected with a commercial glucose meter. These facts

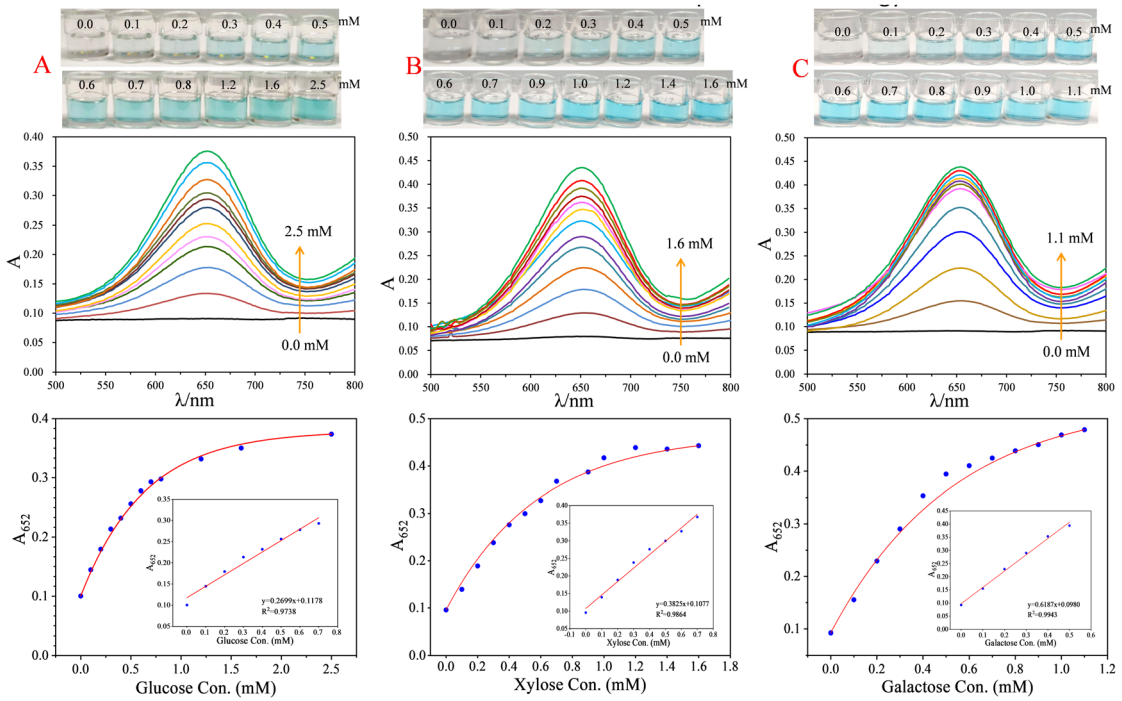

Fig. 3 Photographs, UV-visible spectra and linear relationships between A_{652} and analyte concentrations for detecting different concentrations of glucose (A), xylose (B) and galactose (C) with the corresponding colorimetric method. Data were obtained using the optimal selection described in the text.

validated that the developed method is reliable and thus could be used for the practical detection of glucose in biological samples.

3.4. Bio-enzyme-free colorimetric detection of xylose and galactose based on AuNPs@MoS_2

To further validate the feasibility of AuNPs@MoS_2 as a dual-active nanozyme, we also try to develop colorimetric methods for the detection of xylose and galactose based on AuNPs@MoS_2, respectively. The practicability of experimental strategies was also characterized with UV-visible spectrometry. Like the case of glucose, only the solution containing all of AuNPs@MoS_2, TMB and xylose or galactose exhibited an obvious blue colour and had a maximum adsorption at 652 nm (Fig. S12 in ESI†), indicating that AuNPs@MoS_2 can effectively catalyse the oxidation of xylose or galactose to generate H_2O_2 and then continuously catalyse the H_2O_2-mediated oxidation of TMB since AuNPs@MoS_2 simultaneously possessed peroxidase-like and POx-like activity. The above experimental results verified that the experimental strategy for the colorimetric detection of xylose and galactose is feasible.

The optimal conditions for the colorimetric detection of xylose and galactose were also optimized, respectively, like the case of glucose. The experimental results revealed that the optimal conditions for detecting xylose and galactose are the same. As shown in Fig. S13 (see ESI†), under 40 μL of AuNPs@MoS_2, room temperature as the reaction temperature and 20 min of reaction time between AuNPs@MoS_2 and xylose or galactose, 0.6 mM of TMB, and 40 °C of reaction temperature and 40 min of reaction time between AuNPs@MoS_2 and TMB, the developed colorimetric methods have the highest sensitivity and better stability for the detection of xylose and galactose, respectively.

Under the above optimal conditions, a series of xylose and galactose solutions were detected using the developed method to investigate the analytical performance of the xylose and galactose detection methods, respectively. From Fig. 3B, it can be clearly observed that the solution changed from colourless to deep blue step by step with the increasing xylose concentration from 0.0 mM to 1.6 mM. The colour change of the solution corresponding to 0.3 mM xylose could be clearly identified by naked-eye observation, *i.e.* the visual detection limit of the method is about 0.3 mM for xylose. The absorbance of the system at 652 nm (A_{652}) showed a good linear correlation with the xylose concentration within 0.0–0.70 mM, with a regression equation of $A_{652} = 0.3825 \times C + 0.1077$ ($R^2 = 0.9864$, C is xylose concentration with unit of mM). The LOD ($3\sigma/S$) for xylose was calculated to be 8.0 μM, and the RSD ($n = 5$) for the detection of 0.3 mM xylose was calculated to be 3% (Table S2 in ESI†).

In the case of galactose, as shown in Fig. 3C, the solution also changed from colourless to deep blue step by step upon the increasing galactose concentration from 0.0 mM to 1.1 mM. The colour change of solution corresponding to 0.2 mM galactose could be clearly identified by naked-eye observation, *i.e.* the visual detection limit of the method is about 0.2 mM for galactose. The absorbance of the system at 652 nm (A_{652}) showed a good linear correlation with the galactose concentration within

Table 1 Analytical results of glucose in serum, xylose in bread, and galactose in milk

Sample	Analyte	Added con. (mM)	Bare eye observation	Detected con.[d] (mM)	Rec. (%)	RSD (%)	Glucose meter[e] (mM)
		0.0[a]		0.082	—	4	4.5 (0.09)
Serum	Glucose	0.3[a]		0.385	101	2	—
		0.5[a]		0.527	89	3	—
		0.0[b]		<LOD	—	3	—
Bread	Xylose	0.2[b]		0.178	89	4	—
		0.3[b]		0.324	108	3	—
		0.0[c]		0.095	—	4	—
Milk	Galactose	0.2[c]		0.281	93	3	—
		0.4[c]		0.515	105	4	—

[a] The concentrations of glucose added in final diluted serum, which is used for colorimetric detection. [b] The concentrations of xylose added in the diluted extract of bread, which is used for colorimetric detection. [c] The concentrations of galactose added in final diluted milk, which is used for colorimetric detection. [d] The concentration of analyte in the final diluted solution obtained with our method. [e] The concentration of glucose in original serum and final diluted serum (data in parentheses) obtained with a commercial glucose meter.

0.0–0.50 mM, with a regression equation of $A_{652} = 0.6187 \times C + 0.0980$ ($R^2 = 0.99434$, C is galactose concentration with unit of mM). The detection limit ($3\sigma/S$) for galactose was calculated to be 5.0 μM, and the RSD ($n = 5$) for the detection of 0.2 mM galactose was calculated to be 2% (Table S2 in ESI†).

The xylose in bread samples, which is provided for diabetics, was detected to verify the applicability and the anti-interference ability of the developed xylose detection method, and the galactose in milk samples was detected to verify the applicability and the anti-interference ability of the developed galactose detection method by considering that main pyranose in milk is galactose. The results showed that the xylose in the bread extract can be directly detected without interference, whereas proteins and fat in the original milk will interfere with the detection of galactose in the original milk. Thus, the proteins and fat in milk should be simply removed according to the procedure in the experimental section 2.5 before detection. As shown in Table 1, the xylose in bread can be detected by the proposed method with a recovery of 89–108% and a RSD ($n = 5$) < 5%, and the galactose in the pre-treated milk can be detected by the proposed method with a recovery of 93–105% and a RSD ($n = 5$) < 5%. All the above facts validated that the developed xylose detection method and galactose detection method are reliable and thus could be used for the practical detection of xylose and glucose in food samples, respectively.

As we mentioned above, to date, several bio-enzyme-free colorimetric methods have been developed for the detection of glucose based on the nanozymes with peroxidase-like and GOx-like activities,[23–33] whereas the bio-enzyme-free colorimetric methods for the detection of xylose and galactose were not reported due to the lack of nanozymes with peroxidase-like and POx-like activities. In this study, we first reported the nanozyme with peroxidase-like and POx-like activities simultaneously and further developed the colorimetric methods for the detection of glucose, xylose and galactose, respectively, based on the dual-active nanozyme. The developed bio-enzyme-free colorimetric method for the detection of glucose has similar or higher sensitivity and stability compared to previous bio-enzyme-free colorimetric methods.[23–33]

4. Conclusions

In summary, we herein first prepared a dual-active nanozyme by loading AuNPs on MoS_2 nanosheets (AuNPs@MoS_2). The prepared AuNPs@MoS_2 simultaneously possessed enhanced and stable peroxidase-like and POx-like activities and thus can be used to highly efficiently catalyse the cascade reactions of pyranose (glucose, xylose and galactose) oxidation, such as the tandem reactions of pyranose (glucose, xylose and

galactose) oxidation and H_2O_2-mediated oxidation of TMB, which provides a promising approach for bio-enzyme-free visual detection of glucose, xylose and galactose. Based on the dual enzyme-like activity of AuNPs@MoS_2, we further developed bio-enzyme-free colorimetric methods for the detection of glucose, xylose and galactose, respectively, with a visual detection limit of 0.2–0.3 mM and a spectrometry detection limit of 5.0–11 μM. The developed glucose, xylose and galactose colorimetric detection methods have been successfully used to detect glucose in serum, xylose in bread and galactose in milk, respectively, with a recovery of 89–108% and an RSD (n = 5) < 5%. With enhanced peroxidase-like and POx-like activities simultaneously, and good stability, the developed AuNPs@MoS_2 provided a promising nanozyme for catalysing the cascade reactions of the oxidation of various monosaccharides with pyranyl rings and for fabricating cost-effective, sensitive and simple bio-enzyme-free colorimetric sensors for the visual detection of various monosaccharides with pyranyl ring including glucose, xylose and galactose.

Author contributions

Prof. F.-F. Fu and Dr X. Zhang performed the experimental design, data analysis and interpretation, and manuscript writing. S.-L. Fu, J.-F. Liu, S.-Q. Wu and L. Zhang performed the experiments. The manuscript was written with the contributions of all authors, and all authors have given approval to the final version of the manuscript.

Conflicts of interest

There are no conflicts to declare.

Acknowledgements

The authors gratefully acknowledge the National Natural Science Foundation of China (22276032) and Fujian Provincial Department of Science and Technology (2023Y0005) for financial support.

References

1 X. Zhang, C.-C. Sun, R.-L. Li, X. Jin, Y.-N. Wu and F.-F. Fu, *Anal. Chem.*, 2023, **95**, 5024.
2 H.-Y. Song, C.-L. Ma, L. Wang and Z.-G. Zhu, *Nanoscale*, 2020, **12**, 19284.
3 H. Wei and E.-K. Wang, *Chem. Soc. Rev.*, 2013, **42**, 6060.
4 X.-Y. Wang, Y.-H. Hu and H. Wei, *Inorg. Chem. Front.*, 2016, **3**, 41.
5 W.-Y. Yin, J. Yu, F.-T. Lv, L. Yan, L.-R. Zheng, Z.-J. Gu and Y.-L. Zhao, *ACS Nano*, 2016, **10**, 11000.
6 J. Yu, D.-Q. Ma, L.-Q. Mei, Q. Gao, W.-Y. Yin, X. Zhang, L. Yan, Z.-J. Gu, X.-Y. Ma and Y.-L. Zhao, *J. Mater. Chem. B*, 2018, **6**, 487.
7 X.-H. Xia, J.-T. Zhang, N. Lu, M. J. Kim, K. Ghale, Y. Xu, E. McKenzie, J.-B. Liu and H.-H. Ye, *ACS Nano*, 2015, **9**, 9994.
8 X. Zhu, L. Gao, L. Tang, B. Peng, H.-W. Huang, J.-J. Wang, J.-F. Yu, X.-L. Ouyang and J.-S. Tan, *Biosens. Bioelectron.*, 2019, **146**, 111756.
9 M.-Y. Shi, M. Xu and Z.-Y. Gu, *Anal. Chim. Acta*, 2019, **1079**, 164.
10 A. Koyappayil, S. Berchmans and M.-H. Lee, *Colloids Surf., B*, 2020, **189**, 110840.
11 C.-Y. Liu, Y.-Y. Cai, J. Wang, X. Liu, H. Ren, L. Yan, Y.-J. Zhang, S.-Q. Yang, J. Guo and A.-H. Liu, *ACS Appl. Mater. Interfaces*, 2020, **12**, 42521.
12 M. Comotti, C. Della Pina, R. Matarrese and M. Rossi, *Angew. Chem., Int. Ed.*, 2004, **43**, 5812.
13 W.-J. Luo, C.-F. Zhu, S. Su, D. Li, Y. He, Q. Huang and C.-H. Fan, *ACS Nano*, 2010, **4**, 7451.
14 N. J. Lang, B.-W. Liu and J.-W. Liu, *J. Colloid Interface Sci.*, 2014, **428**, 78.
15 J.-X. Chen, W.-W. Wu, L. Huang, Q. Ma and S.-J. Dong, *Chem. – Eur. J.*, 2019, **25**, 11940.
16 H.-Y. Wang, W.-P. Yang, X.-X. Wang, L.-N. Huang, Y.-Y. Zhang and S.-Z. Yao, *Sens. Actuators, B*, 2020, **304**, 127389.
17 S. Rashtbari, G. Dehghan and M. Amini, *Anal. Chim. Acta*, 2020, **1110**, 98.
18 J. Reiter, H. Strittmatter, L. O. Wiemann, D. Schieder and V. Sieber, *Green Chem.*, 2013, **15**, 1373.
19 O. I. Wilner, S. Shimron, Y. Weizmann, Z.-G. Wang and I. Willner, *Nano Lett.*, 2009, **9**, 2040.
20 J.-L. Fu, M.-H. Liu, Y. Liu, N. W. Woodbury and H. Yan, *J. Am. Chem. Soc.*, 2012, **134**, 5516.
21 Y.-H. Lin, L. Wu, Y.-Y. Huang, J.-S. Ren and X.-G. Qu, *Chem. Sci.*, 2015, **6**, 1272.
22 Y.-Y. Huang, Y.-H. Lin, X. Ran, J.-S. Ren and X.-G. Qu, *Chem. – Eur. J.*, 2016, **22**, 5705.
23 L. Jiao, W.-Q. Xu, H.-Y. Yan, Y. Wu, W.-L. Gu, H. Li, D. Du, Y.-H. Lin and C.-Z. Zhu, *Chem. Commun.*, 2019, **55**, 9865.
24 L.-L. Zhang, J. Pan, Y. Long, J. Li, W. Li, S.-Y. Song, Z. Shi and H.-J. Zhang, *Small*, 2019, **15**, 1903182.
25 Y. Huang, M.-T. Zhao, S.-K. Han, Z.-C. Lai, J. Yang, C.-L. Tan, Q.-L. Ma, Q.-P. Lu, J.-Z. Chen, X. Zhang, Z.-C. Zhang, B. Li, B. Chen, Y. Zong and H. Zhang, *Adv. Mater.*, 2017, **29**, 1700102.
26 Y.-H. Lin, Z.-H. Li, Z.-W. Chen, J.-S. Ren and X.-G. Qu, *Biomaterials*, 2013, **34**, 2600.
27 H.-J. Zhang, X. Liang, L. Han and F. Li, *Small*, 2018, **14**, 1803256.
28 Y.-Y. Zhao, J. Yang, G.-Y. Shan, Z.-Y. Liu, A. Cui, A.-L. Wang, Y.-W. Chen and Y.-C. Liu, *Sens. Actuators, B*, 2020, **305**, 127420.
29 S. Hu, Y.-N. Jiang, Y.-P. Wu, X.-Y. Guo, Y. Ying, Y. Wen and H.-F. Yang, *ACS Appl. Mater. Interfaces*, 2020, **12**, 55324.
30 K. Pramanik, P. Sengupta, B. Majumder, P. Datta and P. Sarkar, *ACS Appl. Mater. Interfaces*, 2020, **12**, 36948.
31 P. Sengupta, K. Pramanik, P. Datta and P. Sarkar, *Biosens. Bioelectron.*, 2020, **154**, 112072.
32 P. Zhang, D.-R. Sun, A. Cho, S. Weon, S. Lee, J. Lee, J. W. Han, D.-P. Kim and W. Choi, *Nat. Commun.*, 2019, **10**, 940.

33 A. R. Deshmukh, H. Aloui and B. S. Kim, *Chem. Eng. J.*, 2021, **421**, 127859.
34 A. T. Abrera, L. Sützl and D. Haltrich, *Bioelectrochemistry*, 2020, **132**, 107409.
35 M.-Z. Li, H. Deng, R. Ma, H.-Y. Luo, B. Yao and X.-Y. Su, *AMB Express*, 2018, **8**, 38.
36 T.-M. Chen, H. Zou, X.-J. Wu, C.-C. Liu, B. Situ, L. Zheng and G.-W. Yang, *ACS Appl. Mater. Interfaces*, 2018, **10**, 12453.
37 T.-R. Lin, L.-S. Zhong, L.-Q. Guo, F.-F. Fu and G.-N. Chen, *Nanoscale*, 2014, **6**, 11856.
38 J. Yu, D.-Q. Ma, L.-Q. Mei, Q. Gao, W.-Y. Yin, X. Zhang, L. Yan, Z.-J. Gu, X.-Y. Ma and Y.-L. Zhao, *J. Mater. Chem. B*, 2018, **6**, 487.
39 N. Wu, Y.-T. Wang, X.-Y. Wang, F.-N. Guo, H. Wen, T. Yang and J.-H. Wang, *Anal. Chim. Acta*, 2019, **1091**, 69.
40 X. Jin, Y.-Y. Zhong, L. Chen, L.-J. Xu, Y.-N. Wu and F.-F. Fu, *Part. Part. Syst. Charact.*, 2018, **35**, 1700359.
41 K. Zhao, W. Gu, S.-S. Zheng, C.-L. Zhang and Y.-Z. Xian, *Talanta*, 2015, **141**, 47.
42 L.-C. He, Q.-Q. Ni, J. Mu, W.-P. Fan, L. Liu, Z.-T. Wang, L. Li, W. Tang, Y.-J. Liu, Y.-Y. Cheng, L.-G. Tang, Z. Yang, Y. Liu, J.-H. Zuo, W.-J. Yang, O. Jacobson, F. Zhang, P.-T. Huang and X.-Y. Chen, *J. Am. Chem. Soc.*, 2020, **142**, 6822.
43 T.-T. Zhu, L.-Y. Huang, Y.-H. Song, Z.-G. Chen, H.-Y. Ji, Y.-P. Li, Y.-G. Xu, Q. Zhang, H. Xu and H.-M. Li, *New J. Chem.*, 2016, **40**, 2168.